Chemistry of Heterocyclic Compounds, Vol. 37, No. 2, 2001

THE EFFECT OF *cis-trans* ISOMERISM ON THE ELECTRONIC–VIBRATIONAL STRUCTURE OF THE GROUND AND EXCITED STATES AND REACTIVITY OF 2-(2-FURYL)- AND 2-(2-THIENYL)OXAZOLE

A. E. Obukhov[1] and L. I. Belen'kii[2]

*The fluorescent properties, structure, and electronic structure of the ground and excited singlet and triplet electronic states of the cis and trans forms of 4,5-dihydro-2-(2-furyl)oxazole, 4,4-dihydro-2-(2-thienyl)oxazole, 2-(2-furyl)oxazole (**FO**), and 2-(2-thienyl)oxazole (**TO**) have been studied. The orbital nature of the lower excited singlet and triplet states has been studied by the semiempirical INDO/S (valence approximation) and PPP/S (π approximation) methods. It was shown that for **FO** and **TO** molecules the lower triplet state is of the $\pi\pi^*$ type, for which delocalization of the electronic excitation on atoms is characteristic. In the singlet excitation state inversion was observed of the energy levels of the delocalized $\pi\pi^*$ states and $n\pi^*$ states localized over several bonds (for the free **TO** and **FO** molecules the lower excited singlet states S_1^* were assigned to $\pi\pi^*$ and $n\pi^*$ types respectively). Owing to the low position of the $T_{\pi\pi}^*$ and $T_{n\pi}^*$ levels relative to the singlet level of $\pi\pi^*$ type, the rate constant for intercombination conversion is greater than the rate constant for radiative decay. Consequently an efficient population of the triplet states of the molecules occurs under conditions of electronic-vibrational excitation. The direction of reactions during synthesis was compared with the localization indices in the ground state for electrophilic, nucleophilic, and radical substitution, and also with the excitation localization numbers L_μ for a wide selection of electronically excited states. It was concluded that the change in the structure of the azole molecule on replacing an O atom by an S atom, or on changing from a partially hydrogenated to a heteroaromatic system, was the main reason for the change of all the spectral parameters characterizing the electronic-vibrational or the spin-orbital interaction of the most reactive groups of atoms in the molecular structure.*

Keywords: 4,5-dihydro-2-(2-thienyl)oxazole, 4,5-dihydro-2-(2-furyl)oxazole, 2-(2-furyl)oxazole, 2-(2-thienyl)oxazole; *s-cis* and *s-trans* forms, fluorescent properties, chemical structure and electronic structure of ground and electronic excited singlet and triplet states, quantum-chemical calculations.

---

[1] Russian Peoples' Friendship University, Moscow 117302; e-mail: aobukhov@mx.pfu.edu.ru.
[2] N. D. Zelinsky Institute of Organic Chemistry, Russian Academy of Sciences, Moscow 117913; e-mail: lb@1september.ru. Translated from Khimiya Geterotsiklicheskikh Soedinenii, No. 2, pp. 187-212, February, 2001. Original article submitted May 12, 2000.

 0009-3122/01/3702-0170$25.00

While studying the interconnection of structure, fluorescence properties, and reactivity of certain 2-substituted oxazoles differing in the nature of the substituent, *viz*. 2-phenyloxazole (**PO**), 2-(2-furyl)oxazole (**FO**), and 2-(2-thienyl)oxazole (**TO**), only the energetically most favorable conformers of the two latter systems were considered. These were the *s-trans* forms of **FO** and **TO** in their ground and lower excited singlet and triplet states [1-3]. The present paper is devoted to a study of the dependence of the reactivity and electronic structure in the ground and electronic excited singlet and triplet states of 2-(2-furyl)oxazole and 2-(2-thienyl)oxazole on their steric structure. The compounds indicated are intermediates in the course of a directed synthesis of laser-active substances [4]. The problem of the investigation was formulated in detail by us in [2,3].

Quantum-chemical calculations were carried out by the semiempirical PPP/S and INDO/S methods for the two possible planar conformers of the molecules using spectral parameters. The methods of calculation have been described in detail in [2].

1. CHANGE IN THE DIRECTION OF ELECTROPHILIC SUBSTITUTION

The data obtained by us show that under conditions excluding protonation or complex formation with a Lewis acid the oxazole nucleus in 2-phenyl, 2-(2-thienyl)- and 2-(2-furyl)oxazoles behaves like an activated five-membered heteroaromatic system with one heteroatom towards electrophilic reagents. It is brominated by bromine without a catalyst, it is nitrated with acetyl nitrate and with N-nitropicolinium fluoroborate, and even undergoes Vilsmeier formylation [4-6]. Neither the benzene nor the thiophene rings are affected but in the case of **FO** a mixture was obtained of products of substitution in the oxazole or furan fragments. Protonation or complex formation (complexes with $AlCl_3$ were studied) occurs at the "pyridine" nitrogen atom [7,8] and leads to deactivation of the oxazole ring so that reaction is directed only to the phenyl (hetaryl) fragment (see scheme).

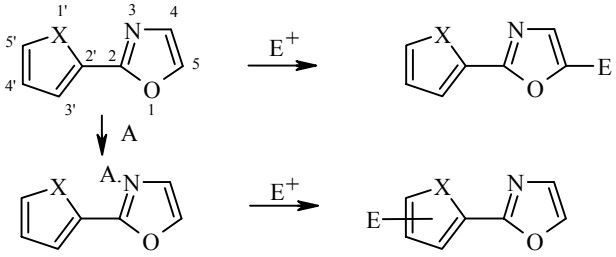

X = CH=CH, S, O; A = H^+, $AlCl_3$

2. REACTIVITY INDICES OF THE INDIVIDUAL POSITIONS OF THE MOLECULES IN THE GROUND STATE

The free valence indices (FV) and frontier electron densities (FED) for the azocyclic molecules in three types of model reactions, *viz*. electrophilic FED(E), nucleophilic FED(N), and radical FED(R) substitution, are given in Table 1. These were calculated by the PPP/S method. These values show the significant differences in the direction of the types of reaction mentioned.

In the case of 2-(2-furyl)oxazole, the FV indices for *cis*-**FO** (*trans*-**FO**) fall in the sequence C(5) > C(5') > C(3') > C(4) > C(4') > C(2') > C(2), but for *cis*-**TO** (*trans*-**TO**) the S and C(5') atoms of the thiophene ring have the maximum FV indices and the FV index values fall in the series C(5') > S(1) > C(5) > C(4') > C(3') > C(4) > C(2') > C(2).

TABLE 1. Reactivity Indices of Atoms in the Molecules of 2-(2-Furyl)oxazole and 2-(2-Thienyl)oxazole according to the PPP/S Method

Compound	Isomer	Index*	O(1)	C(2)	N(3)	C(4)	C(5)	O(1') S(1')	C(2')	C(3')	C(4')	C(5')
2-(2-Furyl)-oxazole (**FO**)	*cis*-**FO**	FV	0.077	0.240	0.142	0.385	0.511	0.102	0.258	0.413	0.380	0.501
		FED(E)	0.023	0.200	0.151	0.188	0.450	0.002	0.321	0.239	0.069	0.358
		FED(N)	0.165	0.355	0.230	0.001	0.224	0.164	0.258	0.282	0.014	0.306
		FED(R)	0.094	0.277	0.190	0.094	0.337	0.083	0.289	0.260	0.042	0.332
		q_i^o	0.319	0.026	-0.272	0.004	-0.102	0.311	-0.098	-0.045	-0.070	-0.074
	trans-**FO**	FV	0.051	0.240	0.146	0.386	0.506	0.079	0.251	0.416	0.381	0.495
		FED(E)	0.023	0.215	0.145	0.206	0.486	0.003	0.288	0.221	0.082	0.350
		FED(N)	0.166	0.343	0.230	0.000	0.207	0.176	0.285	0.290	0.008	0.295
		FED(R)	0.095	0.279	0.188	0.103	0.337	0.090	0.287	0.255	0.045	0.322
		q_i^o	0.322	0.030	-0.286	0.001	-0.09	0.327	-0.087	-0.082	-0.073	-0.068
2-(2-Thienyl)-oxazole (**TO**)	*cis*-**TO**	FV	0.071	0.223	0.146	0.385	0.510	0.625	0.366	0.466	0.420	0.636
		FED(E)	0.024	0.288	0.146	0.190	0.444	0.001	0.288	0.310	0.078	0.321
		FED(N)	0.098	0.153	0.171	0.001	0.139	0.416	0.393	0.124	0.463	0.463
		FED(R)	0.061	0.176	0.158	0.096	0.291	0.022	0.352	0.351	0.101	0.392
		q_i^o	0.324	0.031	-0.273	0.003	-0.095	0.054	-0.034	0.011	-0.011	-0.010
	trans-**TO**	FV	0.065	0.223	0.144	0.384	0.509	0.599	0.354	0.467	0.419	0.627
		FED(E)	0.022	0.205	0.144	0.189	0.447	0.002	0.264	0.304	0.092	0.330
		FED(N)	0.101	0.150	0.174	0.002	0.138	0.048	0.442	0.394	0.105	0.446
		FED(R)	0.061	0.178	0.159	0.096	0.293	0.025	0.353	0.349	0.098	0.388
		q_i^o	0.328	0.004	-0.273	0.004	-0.092	0.061	-0.009	-0.027	-0.021	0.000

* FV is the free valence index, FED(E), FED(N), and FED(R) are frontier electron densities as indices for electrophilic, nucleophilic, and radical substitution respectively.

For the electrophilic substitution of *cis*-**FO** (*trans*-**FO**) the greatest FED(E) indices belong to the C(5) and C(5') atoms. We note that according to the experimental data of [4] these positions compete on Vilsmeier formylation (see section 1). The C(2) and C(5') atoms possess the greatest FED(N) indices for nucleophilic substitution. Also noteworthy are the high FED(N) indices for the C(2') and C(3') atoms equal to 0.258 (0.285) and 0.282 (0.290), which enable participation of the free position 3 of the furan ring in nucleophilic substitution reactions. In the case of radical substitution the C(5) and C(5') atoms have the highest FED(R) indices.

The C(5) atom is characterized by the highest FED(E) index for the electrophilic substitution of *cis*-**TO** (*trans*-**TO**), which agrees with experimental results [4]. In agreement with the experimental data [4], the FED(E) indices predict that the role of the C(4) atom is not large in electrophilic substitution reactions (see section 1). In the case of nucleophilic substitution, judging by the FED(N) values, the most reactive must be the free positions of the thiophene ring. Transition from the *cis* to the *trans* conformation may be accompanied by a significant increase in the reactivity of position 3 of the thiophene ring. The size of FED(N) grows from 0.124 to 0.442. It follows from the values of the FED(R) indices that competition is possible between the thiophene ring and position 5 of the oxazole ring.

3. COMPARISON OF THE EXPERIMENTAL RESULTS AND QUANTUM-CHEMICAL CALCULATIONS WITH NMR DATA

The parameters of the ^{1}H NMR spectra are given in Table 2. It is evident that the chemical shifts of the H(4) and H(5) protons of the oxazole nucleus for phenyl-, furyl-, and thienyl-substituted derivatives differ little from one another. The spectra of 4,5-dihydro-2-phenyl-, 4,5-dihydro-2-(2-furyl)-, and 4,5-dihydro-2-(2-thienyl)oxazoles (**DHPO**, **DHFO**, and **DHTO**) are typical of monosubstituted benzenes, furans, and thiophenes with electron-withdrawing substituents having a –M–I effect (the oxazoline residue is equivalent to an iminoester substituent). On going over to **PO** and **TO** deshielding of the signals of the benzene and thiophene

TABLE 2. Chemical Shifts (ppm) in the ^{1}H NMR Spectra of 2-Aryl-, 2-Hetaryloxazoles, and 2-Aryl-, and 2-Hetaryl-4,5-dihydrooxazoles

Compound	Oxazoline ring		Oxazole ring		Phenyl, H(3') or *o*-H	2-Furyl, H(4')	2-Thienyl H(5') or *m*-H + *p*-H
	H(4)*	H(5)*	H(4)*[2]	H(5)*[2]			
4,5-Dihydro-2-phenyl-oxazole*[3]	3.97	4.08	—	—	7.76 m (2H)		7.22 m (3H)
4,5-Dihydro-2-(2-furyl)-oxazole*[4]*[5]	4.10	4.20	—	—	7.49 dd	6.97 dd	7.45 dd
4,5-Dihydro-2-(2-thienyl)-oxazole*[3]*[6]	4.07	4.22	—	—	6.87 d	6.38 dd	7.45 d
2-Phenyloxazole*[3]	—	—	7.10	7.53	7.95		7.30 m (3H)
2-(2-Furyl)oxazole*[3]	—	—	7.07	7.51	6.87 dd	6.35 dd	7.45 br. d
2-(2-Thienyl)oxazole*[3]	—	—	7.08	7.55	7.51 dd	6.98 dd	7.32 br. d

* Signals have the form of overlapping multiplets, J_{45} = 7-8 Hz.

*[2] Signals have the form of singlets (CC J_{45} < 1 Hz, not displayed in the ^{1}H NMR spectrum at a frequency of 60 MHz.

*[3] In CCl_4 solution.

*[4] In $CDCl_3$ solution.

*[5] In the furan ring, $J_{3'4'}$ = 3.5, $J_{4'5'}$ = 2.5 Hz.

*[6] In the thiophene ring $J_{3'4'}$ = 4, $J_{3'5'}$ = 1.5, $J_{4'5'}$ = 5.5 Hz.

rings occurs, with the exception of the H(5') signal of the thiophene ring. But in the case of **FO** on the other hand, a strengthening was observed in the shielding of the H(3') and H(4') protons of the furan ring, but the chemical shift of H(5') was unchanged. The reason for these differences is probably the high electronegativity of the heteroatom of the furan ring, which causes a lower transfer of electron density from the furan to the oxazole fragment, and may explain the markedly higher differences in reactivity of **TO** and **FO**, and also **PO** [1,2].

The data of INDO/S calculations (Table 3) showed that in the ground state the C(3') atom of the furan or thiophene ring was characterized by the least electron population. The greatest electron population in these rings was on the C(5') atom. The difference in the values of $\Delta\rho_{\pi z}^{0i}$ may explain the more high field chemical shift of the H(5') proton signals for **TO** compared with **FO**, and also the more low field chemical shift of the H(3') protons in the thiophene ring caused by the greater electron population on the C(3') atom (see above).

The analogous values for the C(4) and C(5) atoms of the oxazole ring in the *cis* and *trans* conformers were $\Delta\rho_{\pi z}^{0i}$ = 0.058 and 0.097 (**FO**) and $\Delta\rho_{\pi z}^{0i}$ = 0.062 and 0.074 (**TO**) respectively. A qualitative agreement therefore emerges between the changes of electron density on the atoms and the values of the chemical shifts of the molecular nuclei. Certain disagreements must be noted probably connected with the impossibility of complete calculation in the mathetical models of the various external influences of the medium on an organic multiatomic system [3].

4. FLUORESCENT CHARACTERISTICS

According to data of X-ray structural analysis systems built from directly linked aromatic and/or heteroaromatic rings are planar in the crystalline state (symmetry of the molecules is no greater than C_s), but in gas phase and in solution in the ground state the energetically most favored are nonplanar conformers with an angle between the rings of less than 35-45° [9]. The UV absorption spectra of the **DHFO**, **DHTO**, **FO**, and **TO** molecules in solution indicate the presence of all types of conformers. One broad and intense long-wave absorption band (LAB) was observed in the UV spectra of the azoles in solution (evidently also in gas phase), the extinction coefficient (ε_{abs}^{max}) of which was fairly high (Fig. 1). The spectral data are given in Table 4.

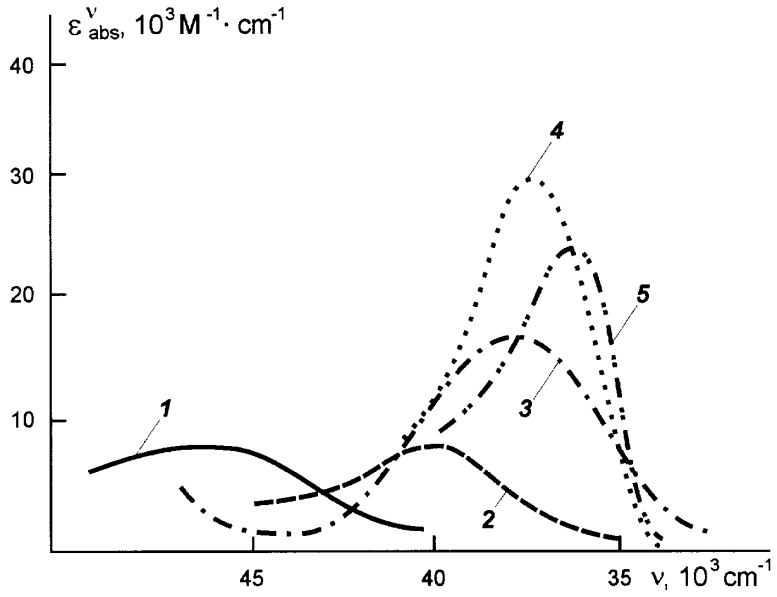

Fig. 1. The UV absorption spectra in ethanol solution of 1) 4,5,4'5'-tetrahydro-2,2'-bioxazole (**THBO**); 2) 4,5-dihydro-2-(2-furyl)oxazole (**DHFO**); 3) 4,5-dihydro-2-(2-thienyl)oxazole (**DHTO**); 4) 2-(2-furyl)oxazole (**FO**); 5) 2-(2-thienyl)oxazole (**TO**).

TABLE 3. Charges q_e, $\Sigma_i q_e$ and the Excitation Localization Numbers L_i, $\Sigma_i L_i$ (%) on Atoms in the Singlet and Triplet Excited States of 2-(2-Furyl)- and 2-(2-Thienyl)oxazole (PPP/S Method) and $\Delta\rho_{\pi}^{0i}$ (INDO/S Method)

Compound	Conformation	Electronic state	Parameter	Atoms										$\Sigma_i q_e$ and $\Sigma_i L_e$ on the atoms of the oxazole ring	Dipole moment *d, D*	Solvation energy M_0^{solv}, kcal/mol
				O(1)	C(2)	N(3)	C(4)	C(5)	O(1') S(1')	C(2')	C(3')	C(4')	C(5')			
1	2	3	4	5	6	7	8	9	10	11	12	13	14	15	16	17
2-(2-Furyl)-oxazole	*cis*-**FO**	S_1*	q_e*	0.249	-0.089	-0.344	0.094	0.018	0.242	-0.043	-0.070	-0.037	-0.019	-0.072	4.7	-42.8
		S_2*		0.288	-0.012	-0.306	0.035	-0.086	0.285	-0.117	-0.032	0.052	-0.107	-0.081	4.3	-49.2
		S_3*		0.265	-0.073	-0.276	0.092	-0.092	0.301	-0.012	0.007	-0.094	-0.119	-0.083	3.8	-47.3
		S_1*	L_i	4.9	15.5	11.0	4.6	15.5	3.6	14.2	13.6	1.9	15.1	51.6		
		S_2*		2.1	5.4	4.9	2.7	5.8	6.6	13.2	18.7	21.2	19.4	20.9		
		S_3*		4.8	10.5	13.1	14.8	15.3	4.0	10.5	12.1	3.2	9.1	61.1		
		T_1	q_e*	0.264	-0.015	-0.256	0.042	-0.069	0.229	-0.058	-0.033	-0.049	-0.056	-0.033	3.9	-35.5
		T_2		0.247	0.041	-0.258	0.036	-0.090	0.269	-0.076	-0.041	-0.056	-0.072	-0.024	4.0	-39.0
		T_3		0.311	0.030	-0.292	-0.018	-0.090	0.318	-0.126	0.008	0.003	-0.145	-0.059	4.4	-56.4
		T_4		0.315	0.012	-0.302	-0.100	0.043	0.334	-0.127	-0.032	-0.047	-0.096	-0.032	5.7	-61.1
		T_5		0.434	-0.268	-0.293	0.262	-0.048	0.319	-0.136	-0.164	-0.028	-0.079	0.087	6.6	-91.8
		T_6		0.302	-0.058	-0.338	0.062	-0.088	0.374	-0.214	-0.342	0.183	0.120	-0.120	8.0	-88.3
		T_1	L_i	3.8	9.8	7.4	44	13.6	4.6	17.8	14.1	5.7	18.9	39		
		T_2		4.8	13.4	2.5	15.7	25.4	2.9	9.1	3.5	8.3	14.5	61.8		
		T_3		1.0	2.1	4.0	5.2	5.4	8.0	13.7	19.8	21.8	18.9	17.8		
		T_4		3.6	20.5	22.0	16.3	16.5	3.8	5.4	7.6	1.4	2.9	78.9		
		T_5		12.3	15.6	24.9	20.2	5.7	2.9	3.0	6.9	4.7	3.8	78.7		
		T_6		2.2	5.2	6.5	5.2	3.4	5.2	10.2	22.5	28.4	11.2	22.5		

TABLE 3 (continued)

1	2	3	4	5	6	7	8	9	10	11	12	13	14	15	16	17
	trans-**FO**	S_1*	q_e*	0.261	-0.072	-0.361	0.105	0.034	0.254	-0.059	-0.124	-0.033	-0.006	-0.033	1.1	-47.0
		S_2*		0.298	-0.006	-0.323	0.044	-0.073	0.292	-0.115	-0.083	0.055	-0.090	-0.059	2.4	-51.7
		S_3*		0.275	-0.053	-0.287	0.068	-0.092	0.314	0.009	-0.017	-0.112	-0.106	-0.088	0.6	-50.0
		S_1*	L_i	5.2	15.4	10.4	5.4	15.8	3.9	14	13.6	2.1	14.3	52.2		
		S_2*		2.2	5.9	4.9	3.1	6.1	6.5	13.5	18.2	20.7	19	22.2		
		S_3*		4.5	12.4	12.1	13.6	14.6	4.2	11.4	13.1	3.9	10.1	57.2		
		T_1	q_e*	0.272	-0.010	-0.270	0.044	-0.063	0.241	-0.056	-0.074	-0.048	-0.049	-0.026	1.1	-37.9
		T_2		0.258	0.047	-0.272	0.036	-0.089	0.281	-0.061	-0.076	-0.056	-0.068	-0.020	1.0	-41.7
		T_3		0.324	0.040	-0.306	-0.025	-0.077	0.327	-0.090	-0.042	-0.036	-0.114	-0.044	2.0	-58.6
		T_4		0.325	0.031	-0.341	-0.103	0.064	0.351	-0.120	-0.065	-0.051	-0.090	-0.025	2.3	-67.2
		T_5		0.431	-0.207	-0.270	0.181	-0.095	0.361	-0.158	-0.255	0.032	-0.019	0.040	0.3	-90.8
		T_6		0.337	-0.114	-0.343	0.128	-0.058	0.361	-0.191	-0.315	0.126	0.067	-0.049	2.8	-84.2
		T_1	L_i	4.0	4.6	7.4	4.6	13.9	4.8	17.4	13.9	5.5	18.3	40.1		
		T_2		4.8	13.0	2.4	15.4	25.0	3.1	9.3	3.6	8.5	14.8	60.6		
		T_3		1.0	2.4	4.2	6.2	6.2	7.0	13.4	19.1	21.5	18.9	20.2		
		T_4		3.1	19.7	20.1	16.8	16.5	4.3	6.2	8.6	1.6	3.0	76.3		
		T_5		11.4	12.6	20.2	13.4	3.8	4.7	6.2	11.1	11.1	5.7	61.3		
		T_6		4.4	8.2	12.0	10.8	4.1	4.3	8.9	17.6	21.3	8.6	39.4		
		S_0	$\Delta\rho_{\pi z}^{0i\ a)}$	-0.191	0.240	0.300	0.058	0.097	-0.203	0.142	-0.028	-0.041	0.106		2.7	
		S_2 ($\pi\pi$*)		0.065	0.054	0.031	-0.071	-0.102	0.046	-0.008	0.052	-0.030	-0.028			
		T_1 ($\pi\pi^*$)		0.073	0.030	-0.007	-0.045	-0.076	0.031	-0.011	0.021	-0.010	-0.006			
2-(2-Thienyl)-oxazole	*cis*-**TO**	S_1*	q_e*	0.283	0.023	-0.301	0.080	0.040	0.038	-0.067	-0.035	-0.013	-0.046	-0.124	4.2	-30.5
		S_2*		0.298	0.010	-0.319	0.013	-0.107	0.589	-0.220	-0.081	0.025	-0.207	-0.106	6.1	-81.0
		S_3*		0.272	0.041	-0.344	0.132	-0.010	0.220	-0.106	0.051	0.001	-0.056	-0.092	5.1	-41.5
		S_4*		0.286	-0.130	-0.297	0.110	0.017	0.128	0.091	0.127	-0.213	-0.118	-0.014	4.8	-41.4
		S_1*	L_i	3.1	9.1	9.0	4.1	13.0	1.2	18.0	17.6	5.2	19.6	38.4		
		S_2*		1.4	2.5	3.3	0.8	3.3	28.9	13.5	15.2	14.1	16.9	11.3		
		S_3*		3.0	10.9	6.6	8.6	12.2	10.1	16.2	12.5	4.4	15.5	41.3		
		S_4*		4.0	14.6	7.8	5.8	11.2	4.6	12.1	10.4	12.6	17.0	43.3		
		T_1	q_e*	0.311	0.023	-0.266	0.015	-0.079	0.032	-0.020	0.000	-0.005	-0.011	0.004	3.0	-29.9
		T_2		0.243	0.019	-0.254	0.063	-0.062	0.049	-0.038	0.000	-0.002	-0.020	0.049	2.5	-70.2
		T_3		0.295	0.061	-0.276	0.002	-0.104	0.070	-0.037	0.017	-0.001	-0.026	-0.023	3.2	-29.8
		T_4		0.332	0.039	-0.305	-0.114	0.063	0.069	-0.039	-0.008	-0.012	-0.025	0.014	4.4	-39.0
		T_5		0.386	-0.165	-0.297	0.279	0.021	0.122	-0.100	-0.123	-0.028	-0.097	0.225	7.4	-60.0
		T_6		0.330	-0.033	-0.297	0.044	-0.114	0.683	-0.205	-0.163	-0.064	-0.181	-0.069	7.1	-98.8

TABLE 3 (continued)

1	2	3	4	5	6	7	8	9	10	11	12	13	14	15	16	17
		T_1	L_i	1.7	2.2	4.7	1.0	4.6	1.1	25.8	18.8	12.3	27.7	14.2		
		T_2		5.0	15.0	5.3	10.1	22.5	0.5	3.5	6.5	15.0	16.6	57.9		
		T_3		2.9	5.7	1.6	11.4	15.2	1.7	16.5	18.7	13.0	13.1	36.8		
		T_4		4.3	20.4	22.9	18.9	18.7	1.1	4.4	6.3	0.5	2.5	85.1		
		T_5		7.9	12.1	22.9	22.5	7.3	4.4	5.6	8.1	2.9	6.3	72.6		
		T_6		3.3	3.5	7.2	3.5	2.2	33.3	12.4	11.8	8.7	14.2	19.7		
	trans-**TO**	S_1*	q_e*	0.286	0.028	-0.308	0.088	0.046	0.048	-0.077	-0.090	-0.001	-0.019	0.140	3.4	
		S_2*		0.303	0.009	-0.323	0.010	-0.111	0.718	-0.238	-0.115	-0.011	-0.242	-0.112	2.9	
		S_3*		0.273	0.048	-0.347	0.125	-0.005	0.152	-0.203	-0.203	0.038	0.009	0.095	1.5	
		S_4*		0.298	-0.115	-0.280	0.120	0.013	0.106	0.097	0.097	-0.240	-0.121	0.036	4.6	
		S_1*	L_i	3.3	9.2	8.5	4.5	13.5	1.6	17.9	17.4	5.1	18.9	39.0		
		S_2*		1.4	1.8	3.1	0.6	2.6	35.4	13.8	14.6	11.3	15.5	9.4		
		S_3*		3.0	11.2	6.6	8.4	12.5	6.6	17.2	9.5	5.6	16.2	41.7		
		S_4*		4.0	13.2	7.6	6.2	10.8	3.2	11.8	11.1	13.8	18.3	41.8		
		T_1	q_e*	0.313	0.022	-0.268	0.016	-0.076	0.036	-0.014	-0.026	-0.004	0.001	0.008	—	
		T_2		0.245	0.019	-0.255	0.068	-0.057	0.055	-0.014	-0.038	-0.012	-0.012	0.020	—	
		T_3		0.298	0.057	-0.276	0.006	-0.102	0.081	-0.018	-0.016	-0.017	-0.012	-0.017	—	
		T_4		0.336	0.059	-0.317	-0.118	0.066	0.087	-0.024	-0.049	-0.023	-0.017	0.026	—	
		T_5		0.312	0.008	-0.313	0.002	-0.118	0.802	0.219	-0.215	-0.071	-0.118	-0.109	—	
		T_6		0.412	-0.203	-0.265	0.316	0.023	0.052	-0.079	-0.158	-0.027	-0.070	0.283	—	
		T_1	L_i	1.7	2.3	4.6	1.0	4.8	1.3	25.7	18.8	12.2	27.5	14.6		
		T_2		5.1	15.3	5.4	9.7	22.5	0.6	3.5	6.5	14.9	16.6	57.9		
		T_3		2.9	5.8	1.5	10.7	14.6	2.0	16.9	19.1	13.2	13.3	35.6		
		T_4		4.1	19.4	21.7	20.2	19.4	1.8	4.4	6.2	0.4	2.5	84.8		
		T_5		1.5	1.6	3.2	0.3	1.8	39.4	15.1	12.3	9.4	15.6	8.3		
		T_6		9.8	13.8	27.6	25.4	7.1	0.5	4.3	6.9	0.7	3.9	83.7		
		S_0	$\Delta\rho_{\pi z}^{0i}$ a)	-0.208	0.278	-0.322	0.062	0.074	-0.049	0.051	-0.002	-0.027	0.035		4.6	
		S_1 ($\pi\pi$*)		0.039	0.076	0.038	-0.104	-0.153	0.033	0.014	0.088	-0.033	0.002			
		T_1 ($\pi\pi$*)		0.031	0.036	0.036	-0.050	-0.050	0.021	-0.006	0.047	-0.020	0.016			

a) According to data of the INDO/S method the minus sign in the calculations by the PPP/S method denotes an increase in the electron population relative to the indigenous atom, and in the calculations by INDO/S the deficit of electron population relative to the number of valence electrons on the atom.

For the partially hydrogenated compounds with conjugated bonds, *viz*. 4,5,4',5'-tetrahydro-2,2'-bioxazole (**THBO**), **DHFO**, and **DHTO**, the extinction coefficent of solutions ε_{abs}^{max} was from 7.51×10^{-3} to 18×10^{-3} and was increased significantly on going over to the heteroaromatic bicyclic molecules **FO** and **TO**, where $\varepsilon_{abs}^{max} = 28.3 \times 10^{-3}$ and 24.1×10^{-3} $M^{-1}cm^{-1}$ respectively. This leads to a regular increase in the absorption cross section at the LAB maximum from $\sigma_{13}^{max} \approx 10^{-18}$ to $\sigma_{13}^{max} \approx 10^{-17}$ to 10^{-16} cm^2. On replacing O atom by S (transition from furan ring to thiophene) a displacement of the LAB was observed of $\Delta\lambda_{abs}^{max} = 19$ (**DHFO-DHTO**) and 14 (**FO-TO**) nm and of the fluorescence bands of $\lambda_{osc,fl}^{max} = -20$ nm, but the band for the 0-0 transition was shifted altogether by $\Delta\lambda_{0\text{-}0} = 2$ nm (about 215 cm^{-1}) in comparison with the Stokes shift of $\Delta\lambda_{abs}^{max} = 24$ nm (Table 4, Figs. 2 and 3).

On going over to a bicyclic molecule containing two heteroaromatic fragments not only do the ε_{abs}^{max} and σ_{13}^{max} parameters change by several orders of magnitude but the fluorescence quantum yield (γ) does too. The latter, although remaining very small, is increased by two orders of magnitude from $\gamma = 0.0001\text{-}0.001$ to $\gamma = 0.01\text{-}0.04$. Evidently the change in nature of the azocycle leads to a small reduction in the rate constant for intercombination conversion to $k_{ST} \approx$ 108-109 sec^{-1}, and a corresponding increase in the rate constant for radiative decay from $k_{fl} = (0.001\text{-}0.01) \times 10^9$ to $k_{fl} \approx 0.1 \times 10^9$ sec^{-1}. In addition there is an increase in the regular growth of the stimulated-emission cross section $\sigma_{13}^{osc,max}$ and a weaker increase in the absorption cross section σ_{13}^{max} (Table 4).

In a series of solvents (cyclohexane, toluene, ethanol, DMF, DMSO, diethylene glycol) significant bathochromic shifts of the LAB by $\Delta\lambda_{abs}^{max} = 1\text{-}3$ nm and of the fluorescence band by $\Delta\lambda_{osc,fl}^{max} = 2\text{-}10$ nm are observed, with an increase in dielectric constant and viscosity or associative properties. There were also insignificant changes in γ, k_{fl}, and k_{ST}. The cross section $\sigma_{31}^{osc,max}$ was little changed in the different solvents. Under conditions of complex formation and protonation in an ethanol + H_2SO_4 mixture the spectral properties experienced a different bathochromic shift relative to the solution in alcohol, $\Delta\lambda_{abs}^{max} = 20$ nm (**FO** and **TO**), $\Delta\lambda_{osc,fl}^{max} = 34$ nm (**FO**), and $\Delta\lambda_{osc,fl}^{max} = 24$ nm (**TO**). The values of the parameters γ, k_{fl}, k_{ST}, and $\sigma_{31}^{osc,max}$ were not improved.

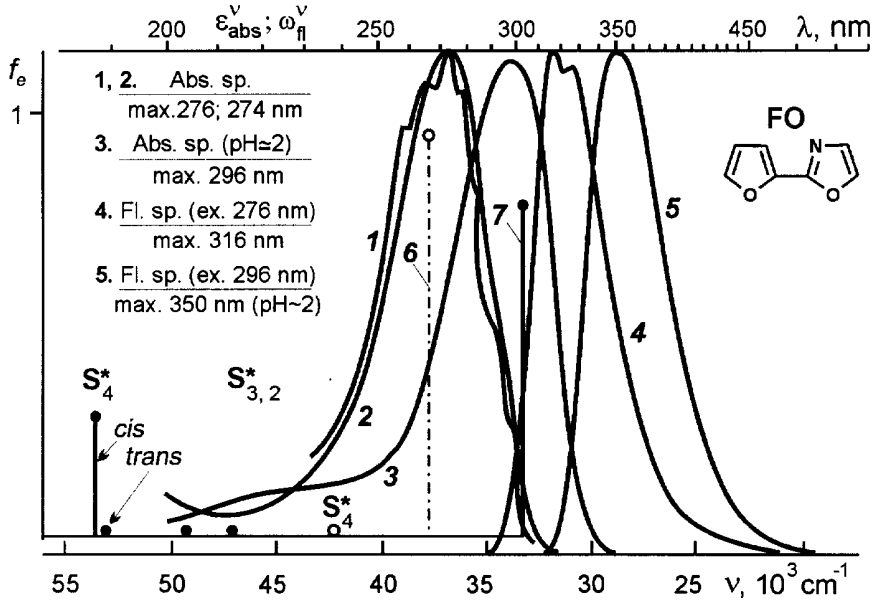

Fig. 2. The UV absorption ε^{ν}_{abs} (1,2,3) and fluorescence ω^{ν}_{fl} spectra (4,5) of solutions of 2-(2-furyl)oxazole (**FO**) in ethanol (3,4), cyclohexane (1), and an ethanol–H_2SO_4 mixture (3,5). The vertical lines (6,7) denote oscillator strengths (f) of the electronic transitions $S_0 \rightarrow S_n^*$, calculated by the PPP/S (7) and INDO/S (6) methods for the *cis* and *trans* conformers.

TABLE 4. Characteristics of the Electronic Absorption Spectra of Oxazole Derivatives in Solution and the Results of Calculations by the INDO/S and PPP/S[a] Methods

Compound	Solvent	ν_{abs}^{max}, cm^{-1}	λ_{abs}^{max}, nm	ν_{fl}^{max}, cm^{-1}	λ_{fl}^{max}, nm	ν_{00}, cm^{-1}	λ_{00}, nm	γ	$\varepsilon_{abs}^{max}\times10^{3}$, $M^{-1}\cdot cm^{-1}$	$k_{fl}\times10^{9}$, sec^{-1}	$k_{ST}\times10^{9}$, sec^{-1}	$\sigma_{13}^{max}\times10^{-16}$, cm^2	$\sigma_{31}^{osc}\times10^{-16}$, cm^2
4,5,4'5'-Tetrahydro-2,2'-bioxazole (**THBO**)	Ethanol	46729	214	—		—	—	0.001	7.5	~0.001	~0.1	<0.03	~0.001
4,5-Dihydro-2-(2-furyl)-oxazole (**DHFO**)	Ethanol	39526	253	—		—	—	0.001	8.7	~0.001	~0.1	<0.004	~0.001
4,5-Dihydro-2-(2-thienyl)-oxazole (**DHTO**)	Ethanol	36765	272					0.01	18.0	0.005	0.50	1.52	0.08
2-(2-Furyl)oxazole (**FO**)	Ethanol	33764	264	31646	350	32680	306	0.04	28.3	0.01	0.23	1.10	0.15
	Ethanol + H_2SO_4	33784	296	28570		30960	323	0.14	27.4	0.2	0.56	0.97	0.49
	calculated:												
	INDO/S	40500	247	32110	311	34710	288	0.01	—	0.088	0.14	1.0	0.004
	PPP/S	40500	247	35300	283	37900	264	0.01	—	0.086	0.21	1.0	0.005
2-(2-Thienyl)oxazole (**TO**)	Ethanol	35461	282	30303	330	32895	304	0.03	24.1	0.003	0.10	0.93	0.53
	Ethanol + H_2SO_4	33784	296	28090	356	34710	326	0.14	22.8	0.4	0.58	0.36	0.56
	calculated:												
	INDO/S	37300	268	32100	288	34700	288	0.01	—	0.055	0.55	0.96	0.007
	PPP/S	36300	275	31100	297	33700	297	0.01	—	0.058	0.58	0.97	0.008

[a] INDO/S and PPP/S are the characteristics of the free molecules calculated by the respective methods, λ_{abs}^{max} (ν_{abs}^{max}), λ_{fl}^{max} (ν_{fl}^{max}), λ_{00} (ν_{00}) are the wavelength (frequency) maxima respectively of UV absorption, fluorescence, and electronic 0-0 transition, ε_{abs}^{max} is the extinction coefficient at the maximum of the UV absorption band, γ is the fluorescence quantum yield, k_{fl} and k_{ST} are the rate constants for radiative decay and intercombination conversion, σ_{13}^{max} and σ_{31}^{osc} (σ_{13}^{fl}) the absorption and stimulated-emission cross sections.

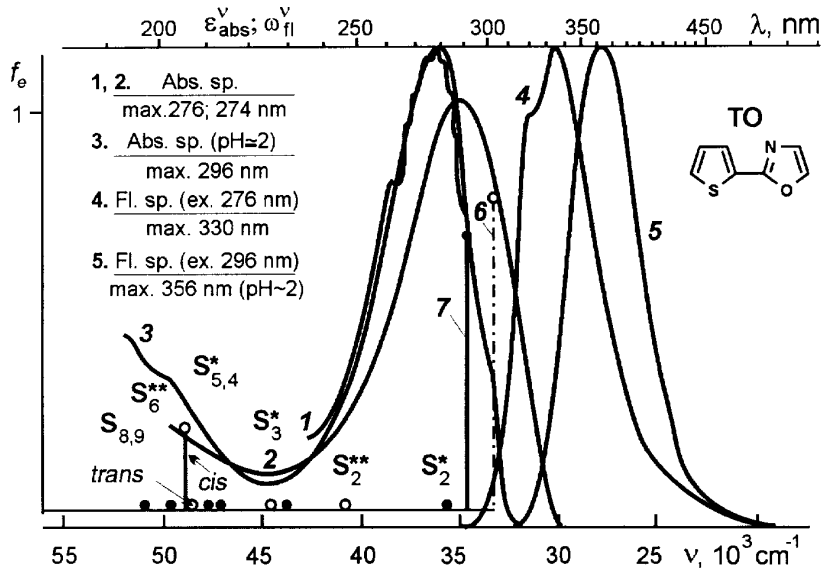

Fig. 3. The UV absorption ε^{ν}_{abs} (1,2,3) and fluorescence ω^{ν}_{fl} (4,5) spectra of solutions of 2-(2-thienyl)oxazole (**TO**) in ethanol (3,4), cyclohexane (1), and an ethanol–H_2SO_4 mixture (3,5). The vertical lines (6,7) denote oscillator strength (f^l) of the $S_0 \rightarrow S_n$* electronic transitions, calculated by the PPP/S (7) and INDO/S (6) methods for the *cis* and *trans* conformers.

Due to the high rates of intercombination conversion the studied molecules only transform efficiently the energy of electronic vibrational excitation in the dark. The triplet states are therefore highly populated.

According to the data of the INDO/S method the highest electron population in the ground state of the **FO** and **TO** molecules is observed on the N atom while a strong reduction of electron density is noted on the O atoms of **FO** molecules and also on the O and S atoms of **TO** molecules (Table 3). It is evident that, even under conditions of a competing increase in electron population on the C atom of the oxazole ring, the presence of an unshared electron pair on the N atom makes it the most probable place for attack on protonation. As previous investigations showed the change in geometry of azoles on protonation is accompanied by a change of all their spectral characteristics [1-3].

5. COMPARISON OF THE TOTAL AND σ- AND π-COMPONENT BINDING ENERGIES OF THE MOLECULES

Calculations by the PPP/S method on **FO** and **TO** molecules show the regular increase of total binding energy $E_{\sigma\pi}^{bond}$ (σπ-electron energy, kcal/mole): -1335.29/-1338.38 = 0.997(7) for *cis*- and *trans*-**FO**; -1241.06/-1241.57 = 0.999(6) for *cis*- and *trans*-**TO**, and also the σ- and π-components of this energy: $E_{\sigma}^{bond}/E_{\sigma}^{bond}$ = -929.71/-894.39 = 1.04 and $E_{\pi}^{bond}/E_{\pi}^{bond}$ = -405.58/-346.67 = 1.17 for *cis*-**FO** and *cis*-**TO**; $E_{\sigma}^{bond}/E_{\sigma}^{bond}$ = -929.69/-894.36 = 1.04 and $E_{\pi}^{bond}/E_{\pi}^{bond}$ = -408.69/-347.21 = 1.18 for *trans*-**FO** and *trans*-**TO**. The total binding energy of the **TO** molecule is therefore less than that of **FO** which is confirmed experimentally by the bathochromic shift of the fluorescence bands (Figs. 4 and 5), but the ratio of the σ and π components of this energy are $E_{\sigma}^{bond}/E_{\pi}^{bond}$ = -929.71/-405.58 = 2.29 and -929.69/-408.69 = 2.28 for *cis*- and *trans*-**FO**; -894.39/-346.67 = 2.58 and -894.36/-347.21 = 2.58 for *cis*- and *trans*-**TO** respectively. Consequently the relative contribution of E_{σ}^{bond} is several times greater than that of E_{π}^{bond} and is conserved in practice in the *cis*-*trans* isomerism, and the contribution is greater for **TO** than for **FO**.

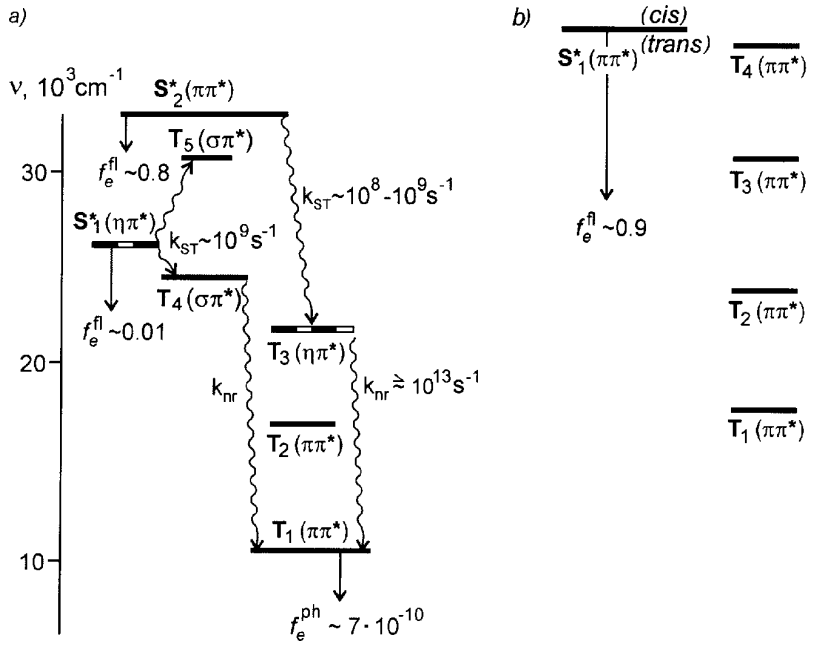

Fig. 4. Diagrams of the electronic singlet S_i* and triplet T_j states and transitions of a free molecule of 2-(2-furyl)oxazole (**FO**) according to a) INDO/S and b) PPP/S. The vertical straight lines denote oscillator strengths for the radiative transitions $S_1^* \rightarrow S_0$ and $T_1 \rightarrow S_0$ and the wavy lines show spin-orbital interacting electronic states of $n\pi^*$, $\pi\pi^*$, and $\sigma\pi^*$ types (k_{ST}, k_{nr} are rate constants for intercombination and internal conversion).

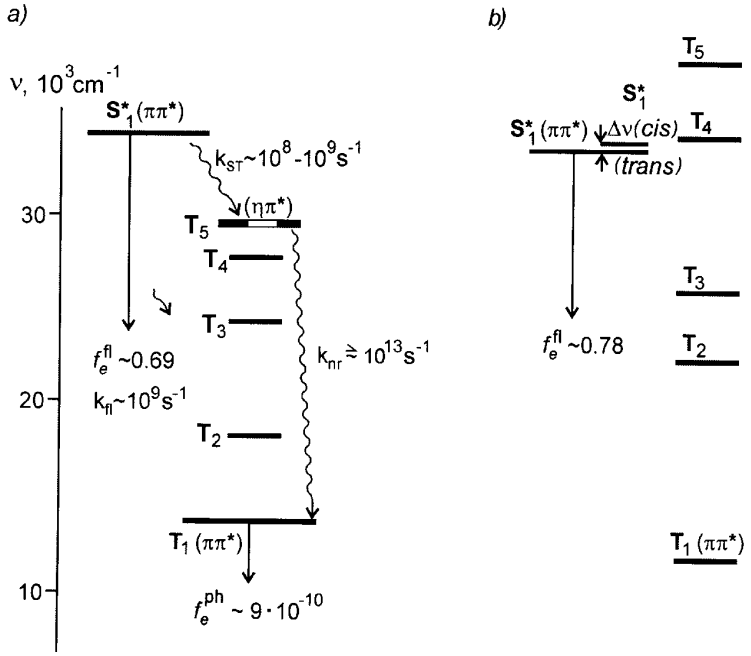

Fig. 5. Diagrams of the electronic singlet S_i* and triplet T_j states and transitions of a free molecule of 2-(2-thienyl)oxazole (**TO**) according to the INDO/S and b) PPP/S methods. The vertical straight lines denote oscillator strengths for the radiative transitions $S_1^* \rightarrow S_0$ and $T_1 \rightarrow S_0$ and the wavy lines show spin-orbital interacting electronic states of nπ*, $\pi\pi^*$, and $\sigma\pi^*$ types (k_{ST}, k_{nr} are rate constants for intercombination and internal conversion).

TABLE 5. Total and π-, σ-Component Binding Energies of Molecules according to PPP/S Data (kcal/mole)

Compound	Isomer	E_π^{bond}	E_σ^{bond}	$E_{\pi+\sigma}^{bond}$	M_0^{solv}
2-(2-Furyl)oxazole	*cis*-**FO**	-405.58	-929.71	-1335.29	45.21
	trans-**FO**	-408.69	-929.69	-1338.38	46.88
2-(2-Thienyl)oxazole	*cis*-**TO**	-346.67	-894.39	-1241.06	26.88
	trans-**TO**	-347.21	-894.36	-1241.57	27.03

A reduction in solvation energy is observed on replacing a furan ring by thiophene (for example, for *cis*-**FO** and *cis*-**TO** M_0^{solv} = -45.21 and -26.88, and for *trans*-**FO** and *trans*-**TO** M_0^{solv} = -46.88 and -27.03 kcal/mole respectively). The values of M_0^{solv} for the *trans* isomers are therefore somewhat greater (Table 5) and consequently their capacity for solvation is higher.

6. ORBITAL NATURE OF THE LOWER EXCITED STATES AND TRANSITIONS

Characteristics are given in Table 3 and diagrams are shown in Figs. 4 and 5 for the excited electronic singlet (S_1*) and triplet (T_j) states of the **FO** and **TO** molecules calculated by the PPP/S and INDO/S methods. It follows from a comparison of Figs. 4 and 5 that by replacing a furan ring (in **FO**) by a thiophene (in **TO**) an inversion is observed of the excited singlet states $S_{1,2}$* of $\pi\pi$* and $n\pi$* types due to an increase in both the energy of the $S1^* \rightarrow S_0$ transition of $\pi\pi$* and $n\pi$* types forbidden by symmetry of more than 7800 cm^{-1} (*trans*-**FO** → *trans*-**TO**) and the energy of the T_1 state by 2800 cm^{-1}. Electronic transitions of the $n\pi$* type were not observed in the UV spectrum of the **FO** molecule.

The presence of a broad and intense LAB indicates that it is formed by vibrational progressions all the terms of which are formed by electronic vibrational transitions of the $\pi\pi$* type.

Transitions of a different orbital nature ($\Delta\lambda_{osc,fl}^{max}$) are masked by the $\pi\pi$* transitions. The difference between the UV spectra calculated by INDO/S and experimentally of **FO** molecules is linked with the action of the solvent on the unshared pair of electrons on the N atom, as a result of which the localization of electron density at the atom is changed in the solvated lower singlet state of the $n\pi$* type and the transition frequency in the experimental spectrum is increased [1].

The $S_{1,2}^* \rightarrow S_0$ fluorescent transition ($\pi\pi$* type) in the *trans*-**FO** and *trans*-**TO** molecules is permitted and is distinguished by the high strength of the oscillator: f_e^{osc} = 0.80 and 0.69 (INDO/S) and f_e^{osc} = 0.90 and 0.78 (PPP/S). According to the PPP/S data for *cis*-**FO** and *cis*-**TO** the oscillator strengths f_e^{osc} were somewhat higher than for the *trans* forms of these molecules and were 0.95 and 0.80 respectively. Transitions from the highly located $S_{3,4,5}$* states are characterized by significantly reduced oscillator strengths (f_e^{osc} = 0.001-0.2) depending on whether the compound is in the *cis* or *trans* form. For example, the intensity of the $S_0 \rightarrow S_4$* transition for the *trans* form was significantly lower than for the *cis* form. For *trans*- and *cis*-**FO** f_e^{osc} = 0.020 and 0.28, for *trans*- and *cis*-**TO** f_e^{osc} = 0.023 and 0.214 respectively. Consequently the observed growth in the intensity of the short wave absorption band (SAB) in the UV spectrum in cyclohexane and in ethanol (Fig. 1) is evidently connected with the predominance of the *cis* form of the molecules, as a result of forming an intramolecular hydrogen bond between the unshared electron pair on the N atom of the oxazole ring and the proton in position 4' of the furan or thiophene ring.

Judging by the UV spectra of solutions and vapors the fraction of *cis*-form for **TO** is greater than for **FO**. In an ethanol + H_2SO_4 mixture the intensities of the SAB for **FO** and **TO** were reduced. This may be linked with the fact that in this mixture instead of an intramolecular a stronger intermolecular hydrogen bond is formed with the nitrogen atom of the **FO** or **TO** molecule. As a result of this the probability of forming the *cis* forms of the molecules is uniformly reduced, due to which the intensity of the SAB falls.

The $T_1 \rightarrow S_0$ ($\pi\pi^*$ type) transitions in the **FO** and **TO** molecules with oscillator strength $f_e^{phosph} \approx 7.4$ and 8.7×10^{-10} are forbidden by symmetry. This is characteristic of the majority of heteroaromatic compounds [3]. In this way the energies of electronic excitation attributed to the triplet state will be most effectively spent in nonoptical transitions.

The fluorescent transitions $S_{1,2}^* \rightarrow S_0$ in the **FO** and **TO** molecules are brought about predominantly from the highest occupied (HOMO) into the lowest unoccupied (LUMO) molecular orbital. The characteristics obtained in the PPP/S method based on atomic orbitals (AO) may be represented in the following way:

cis-**FO** :

$|\psi_{\text{HOMO}\rightarrow\text{LUMO}}|^2 = 0.98$, $E_{\text{HOMO}} = -9.11$ eV, $E_{\text{LUMO}} = -1.36$ eV, $\Delta E_{HOMO\rightarrow LUMO} = 7.75$ eV.

$\psi_{HOMO} = \varphi_{C_4}(0.307) + \varphi_{C_5}(0.474) + \varphi_{O_1}(0.029) + \varphi_{C_2,}(0.401) + \varphi_{C_3,}(0.345)$,

$\psi_{LUMO} = \varphi_{O_1}(0.288) + \varphi_{C_2}(0.339) + \varphi_{N_3}(0.019) + \varphi_{O_1,}(0.287) + \varphi_{C_3,}(0.376) +$

$\varphi_{C_4,}(0.084)$.

trans-**FO**:

$|\psi_{\text{HOMO}\rightarrow\text{LUMO}}|^2 = 0.98$, $E_{HOMO} = -9.14$ eV, $E_{LUMO} = -1.37$ eV, $\Delta E_{HOMO\rightarrow LUMO} = 7.77$ eV.

$\psi_{HOMO} = \varphi_{C_4}(0.321) + \varphi_{C_5}(0.483) + \varphi_{O_1}(0.041) + \varphi_{C_2,}(0.380) + \varphi_{C_3,}(0.332)$,

$\psi_{LUMO} = \varphi_{O_1}(0.288) + \varphi_{N_3}(0.339) + \varphi_{O_1,}(0.297) + \varphi_{C_3,}(0.381) + \varphi_{C_4,}(0.064)$.

cis-**TO:**

$|\psi_{\text{HOMO}\rightarrow\text{LUMO}}|^2 = 0.98$, $E_{HOMO} = -1.98$ eV, $E_{LUMO} = -9.06$ eV, $\Delta E_{HOMO\rightarrow LUMO} = 8.08$ eV.

$\psi_{HOMO} = \varphi_{C_4}(0.380) + \varphi_{C_5}(0.471) + \varphi_{S_1}(0.018) + \varphi_{C_2,}(0.380) + \varphi_{C_3,}(0.394)$,

$\psi_{LUMO} = \varphi_{O_1}(0.276) + \varphi_{C_4}(0.024) + \varphi_{C_5}(263) + \varphi_{C_2,}(0.456) + \varphi_{C_5,}(0.481)$.

trans-**TO**:

$|\psi_{\text{HOMO}\rightarrow\text{LUMO}}|^2 = 0.98$, $E_{HOMO} = -2.03$ eV, $E_{LUMO} = -9.12$ eV, $\Delta E_{HOMO\rightarrow LUMO} = 7.14$ eV.

$\psi_{HOMO} = \varphi_{C_4}(0.307) + \varphi_{C_5}(0.473) + \varphi_{S_1'}(0.031) + \varphi_{C_2,}(0.364) + \varphi_{C_3,}(0.390\ )$

$\psi_{LUMO} = \varphi_{O_1}(0.225) + \varphi_{N_3}(0.295) + \varphi_{S_1,}(0.155) + \varphi_{C_3,}(0.444) + \varphi_{C_4,}(0.229)$.

It follows from the data presented that the greatest contributions to the HOMO are given by the AO of the C(2) and C(5) atoms in the free positions of the oxazole ring and the C(2') and C(3') atoms of the furan ring for the *cis* and *trans* forms of both **FO** and **TO**.

The mutual conversion of the cissoid and transoid conformations (for brevity often called *cis-trans*-isomerization by us) of the **FO** and **TO** molecules has a significant influence on the coefficients in the breakdown of the LUMO on AO. In the case of *cis*-**FO** with the greatest coefficients only the AO of the two carbon atoms and the two oxygen atoms of the oxazole and furan rings, *viz*. C(2), C(3') (max), O(1), and O(1') are taken into consideration. For *cis*-**TO** only the AO of C(2), C(5), C(2'), C(5') (max) are taken, i.e. on replacing the furan ring by thiophene the C(5') atom of the latter remains the most reactive. In the case of *trans*-**FO** the coefficients of the AO of the O(1) and N(3) atoms of the oxazole ring, and also the AO of the C(2') and C(3') atoms of the furan ring, predominantly affect the changes in the breakdown of the LUMO. However in the case of *trans*-**TO**, apart from the AO of the O(1) and N(3) atoms, the AO of the S atom and also other C atoms of the thiophene ring C(3') (max) and C(4') are taken into consideration. It therefore follows that on changing the position of the conformational equilibrium as a result of changing the solvent, temperature, etc., a variation in the position of attack of the reagent, i.e. the direction of the addition-cleavage reaction, is possible.

7. PROPERTIES OF THE EXCITED STATES AND ASSESSMENT OF REACTIVITY

In agreement with the data of [1-3,14] the differences of spectral shifts of the λ_{abs}^{max}, $\lambda_{0\text{-}0}$, and λ_{osc}^{max} bands in the optical spectra indicate a change in the vibronic interactions of the valence bonds in the lower excited states of the **FO** and **TO** molecules, which in its turn must show up in the geometry of their subsystems. Consideration of the data of Table 4 and Figs. 4 and 5 show that the deviations of the frequencies of the electronic 0-0 transition, calculated by the INDO/S and PPP/S methods, from those determined by UV absorption and fluorescence spectra for a solution in cyclohexane (the closest to the optical spectrum of organic molecules in dense vapor [3]) for *cis*-**FO** were: $\Delta\nu_{0\text{-}0} = \nu_{0\text{-}0}^{exp} - \nu_{0\text{-}0}^{theor} = 32680 - 30100 = 1150$ cm^{-1} (INDO/S) and $\Delta\nu_{0\text{-}0} = 32680 - 37893 = -5213$ cm^{-1} (found for *trans*-**FO** by the PPP/S method $\Delta\nu_{0\text{-}0} = 32860 - 37890 = -5210$ cm^{-1}). The differences were also less for *cis*-**TO**: $\Delta\nu_{0\text{-}0} = \nu_{0\text{-}0}^{exp} - \nu_{0\text{-}0}^{theor} = 32895 - 30000 = -2895$ cm^{-1} (INDO/S) and $\Delta\nu_{0\text{-}0} = 32895 - 33664 = -769$ cm^{-1}; for *trans*-**TO** $\Delta\nu_{0\text{-}0} = 32895 - 33482 = -587$ cm^{-1} (PPP/S). Consequently, although the total energies of the *cis* and *trans* conformers of the bicyclic azoles differ little (both in the free state and in solution, which follows from the proximity of the solvation energy values for *cis*- and *trans*-**FO** or *cis*- and *trans*-**TO**), the reactivity of the corresponding positions in the rings may be changed significantly.

8. ELECTRON CHARACTERISTICS OF THE GROUND AND EXCITED STATES

In order to characterize the spectral properties of any multiatomic molecule, this molecule may be represented as a system of quantum-excited electronic states S_i* and T_i. After absorption of a quantum of excitation the electron system of the molecule dissipates the accumulated energy in optical and nonoptical processes. In matrix mechanics these processes are considered as intramolecular relaxations and are described by operators of electronic, vibronic, and spin-orbital interactions (nonadiabaticity operator) [3,10]. The electron and vibronic characteristics of the S_i* and T_j states for the **FO** and **TO** molecules calculated by the INDO/S and PPP/S semiempirical methods [1-3] are given in Table 3.

8.1. Localization of Charges in the Ground State

It follows from the data of Table 3 that the charge distribution q_e and $\Delta\rho_{\pi z}^{0i}$ is substantially local in the molecules being studied. The highest electron density is localized on the N atom. According to the PPP/S data the charge q_e on the N atom is the greatest for *trans*-**FO**, but according to INDO/S the N atom in *cis*-**TO** has highest value of $\Delta\rho_{\pi z}^{0i}$. Replacing the furan ring by thiophene does not change the character of the charge distribution in the oxazole ring in principle, but significantly reduces its electron-donating ability. The overall negative charge on the oxazole ring on changing from *cis(trans)*-**FO** to *cis(trans)*-**TO** is reduced from $\sum q_e = -0.025$ (0.020) to $\sum q_e = -0.010$ (-0.004) (Table 3). This is linked with the sharp fall in the differences in charge q_e on the C atoms for **TO** compared with **FO** and is caused by the presence of the S atom in the **TO** molecule. The negative charge on the C(3') atom in the furan ring is greater than in the thiophene which is in agreement with the stronger displacement towards low field of the H(3') proton signals of the **TO** molecule compared with **FO** (Tables 2 and 3).

8.2. Localization of Charges in Excited States

It follows from the data of Table 5 that on excitation the charge distribution q_e* in the S_1*, S_2*, and T_1 states of the **FO** and **TO** molecules is changed both quantitatively and qualitatively. Since fluorescence of the $\pi\pi$* type is observed from the excited singlet states (S_2* for **FO** and S_1* for **TO**) for the studied compounds, less basic attention will be paid to this state.

The greatest negative charge is localized on the N(3) atom for *cis*(*trans*)-**FO** in the ππ* type S_2* fluorescent state (the electronegativity is increased compared with the ground state). Maximum negative charge on the N(3) atom is also a characteristic of *cis*(*trans*)-**TO** (ππ* type S_1* state). However the charge on the N(3) atom for these compounds is reduced in the ππ* type T_1 phosphorescent state, and this change is significantly more displayed in the case of **FO**.

The charges on the C(3'), C(4'), and C(5') atoms differ significantly in the conformers in the S_1* and S_2* fluorescent states. The trend of the changes of electron population does not coincide in the S_1* and T_1 states. For example, in the T_1 state, in contrast to the S_1* state, for the *trans* forms of **FO** and **TO**, the greatest electron density is localized on the C(3') atom (Table 3).

The character of the changes of q_e* and $\Delta\rho_{\pi z}$* in the more highly situated S_i* and T_j states is significantly different than in the S_1* and T_1 states but the surplus electron density is practically always localized on the N(3) atom. Only one location, the N(3) atom, is therefore possible for attack by reactive proton under conditions of complex formation and protonation (Table 3).

The conformers in the S_0 state possess significantly different dipole moments. For *cis*(*trans*)-**FO** d_0 = 4.81 *D* (1.39 *D*) and for *cis*(*trans*)-**TO** d_0 = 3.26 *D* (2.52 *D*). In the excited S_1* and T_1 states the values of the dipole moment varied. For *cis*(*trans*)-**FO** d_0^S = 4.72 *D* (1.14 *D*) and d_0^T = 3.86 *D* (1.1 *D*); for *cis*(*trans*)-**TO** d_0^S = 4.24 *D* (3.36 *D*) and d_0^T = 3.0 *D* (2.56 *D*). In the more highly situated S_i* and T_j states the dipole moment as a rule grows. The role of orientation effects (dipole-dipole mechanism of intermolecular interaction) essentially grows on excitation of the **FO** and **TO** molecules to any of the electronic S_i* and T_j states. A strong increase was noted in the values of M_0^{solv} both in the singlet and in the triplet states, which indicates an increase in the ability of the studied azoles to become solvated on excitation. For the *trans* forms of the azoles the growth of M_0^{solv} is expressed significantly more strongly, which may be connected with the high steric accessibility of the N atom.

According to PPP/S data, on excitation of the **TO** molecule the size and direction of intramolecular charge transfer (ICT) depends on the level of the S_i* and T_j electronic states. For the electronic states $S_{1,\ldots,4}$ and $T_{1,\ldots,4}$ it is a characteristic of the **FO** molecule that ICT is effected from the furan to the azocycle ring. In this case the oxazole ring is an acceptor and the furan a donor of electrons. For the azocycle of *cis(trans)*-**FO** in the S_2* state $\sum_i q_i$* = -0.081 (-0.059). In the S_1* and T_1 states the azocycle is a weaker acceptor of electron density and for *cis(trans)*-**FO** $\sum_i q_i$* = -0.072 (-0.033) and -0.033 (-0.026) respectively. It should be noted that the azocycle of the *trans* isomer of **TO** in the T_1 state is an even weaker donor of electrons ($\sum_i q_i$* = 0.008). Since in the T_1 state the size of $\sum_i q_i$* is significantly less, then the electronic-vibrational fluorescent S_1* $\rightarrow$ S_0 transition in the excited **FO** molecule is more delocalized than the phosphorescent T_1 $\rightarrow$ S_0 transition. It is therefore characteristic of the *cis* and *trans* isomers of **FO** that the change in spin of the electron system influences not only the size of the ICT, but also its direction.

In the case of *cis(trans)*-**TO** in the S_0 ground state and in the excited T_1 state the oxazole ring is almost electroneutral, i.e. the **TO** molecule is practically unpolarized and is strongly polarized only in the S_1* state, $\sum_i q_i$* = 0.124 (0.140). The structural variations in the studied molecules (replacement of the furan ring by thiophene or *cis-trans* isomerization) therefore change the electronic characteristics of the excited states of different spin and orbital nature.

8.3. Localization Numbers of Electronic Excitation

The localization number L_i of electronic excitation on atoms and subsystems $\sum_i L_\mu$ in the S_i* and T_j excited states of molecules calculated by the PPP/S method are given in Table 3.

Analysis of the distribution of localization numbers L_i according to atom shows that in the *cis(trans)* isomers of **FO** the most reactive are positions 2, 3, and 5 of the oxazole and 2', 3', and 5' of the furan ring: in the oxazole ring of the free molecule in the S_1* state for atoms C(2), N(3), and C(5) L_i = 15.5 (15.4), 11.0 (10.4),

and 15.5 (15.8)%, and in the T_1 state L_i = 9.8 (4.6), 7.4 (7.4), and 13.6 (13.9)% respectively: in the furan ring for atoms C(2'), C(3'), and C(5') in the S_1* state L_i = 14.2 (14.0), 13.6 (13.6), and 15.1 (14.3)%, and in the T_1 state L_i = 17.8 (17.4), 14.1 (13.9), and 18.9 (18.3)%. It must therefore be noted that judging by these localization numbers the reactivity of the furan ring of the **FO** molecule is comparable with that of the benzene ring in 2-phenyloxazole (for the *para* position L_i = 14.0% [2]).

On replacing the furan ring by thiophene the relative reactivity of the individual positions (atoms of the subsystem) is changed markedly. For *cis(trans)*-**TO** the localization numbers L_i show that in the free molecule in the S_1* state positions 2, 3, and 5 of the oxazole ring are the most reactive: for atoms C(2), N(3), and C(5) L_i = 9.1 (9.2), 9.0 (8.5), and 13.0 (13.5)%. These values are sharply reduced in the T_1 state, L_i = 2.2 (2.3), 4.7 (4.6), and 4.6 (4.8)% respectively. However the greatest reactivity was possessed by atoms C(2'), C(3'), and C(5') of the thiophene ring: in the S_1* state L_i = 18.0 (17.9), 17.6 (17.4), and 19.6 (18.9)%, and in the T_1 state L_i = 25.8 (25.5), 18.8 (18.8), and 27.7 (27.5)%. The α-position of the thiophene ring in the **TO** molecule in the lower triplet T_1 state is seemingly significantly more reactive than the C atoms of the furan ring of the free **FO** molecule.

In *cis(trans)*-**FO** the overall percentage localization of excitation on the oxazole ring is significantly different for the various states: $\sum_i L_\mu$ = 51.6 (52.2) (S_1*), 20.9 (22.2) (S_2*), and 39.0 (40.1) (T_1)%, i.e. depending on the spin of the excited state a differently directed reaction is possible due to the different character of localization of electronic-vibrational excitation.

On going from **FO** to **TO** a significant redistribution of $\sum_i L_\mu$ is observed. For *cis(trans)*-**TO** in the S_1* state the excitation is localized mainly in the thiophene fragment and $\sum_i L_\mu$ = 61.6 (61)%. In the T_1 state the thiophene fragment is still characterized by a larger percentage of excitation: $\sum_i L_\mu$ = 85.8 (85.4)%, i.e. in the lower triplet state the reactivity of the thiophene fragment of **TO** must be higher. In the more highly situated S_i* and T_j states of the $\pi\pi$* type the character of the localization of excitation is sharply reduced, which is shown by the values of L_μ and $\sum_i L_\mu$ (see Table 3).

The distribution of indices L_i in the T_1 triplet state is probably more reliable, since according to fluorescence spectroscopy the intercombination conversion of the population of the more long-lived triplet states for the bicyclic molecules occurs at the greatest rate (section 4).

8.4. Geometry of Molecules, Bond Orders, and Electronic-vibrational Processes in the Excited States with Different Spins

Values are given in Table 6 for the lengths and orders of the valence bonds in **FO** and **TO** obtained on optimizing the geometry by the PPP/S method and taken from experimental data for the related compounds POPOP (X-ray structural analysis) [11], 2,5-diphenyl-1,3,4-oxadiazole (electronography) [9], thiophene (microwave spectra [12], electronography [13]). In the oxazole ring of *cis(trans)*-**FO** and 2-phenyloxazole the optimized lengths of the single bonds O(1)–C(2), N(3)–C(4), C(5)–O(1) {$l_{\mu\nu}$ = 1.314 (1.315), 1.347 (1.346), 1.321 (1.321) Å and $l_{\mu\nu}$ = 1.314, 1.346 and 1.321 Å [2] respectively} are less than the experimental values used in the INDO/S method $l_{\mu\nu}$ = 1.360, 1.384, and 1,378 Å (X-ray), but the double bonds C(2)=N(3) and C(4)=C(5) on the other hand are longer: $l_{\mu\nu}$ = 1.323 and 1.377 Å (optimization) and $l_{\mu\nu}$ = 1.294 and 1.347 Å (X-ray). The optimized bond lengths in the furan ring of **FO** are underestimated compared with experimental values but reflect their character accurately. For example, for the single bonds O(1')–C(2') and C(5')—O(1') $l_{\mu\nu}$ = 1.321 and 1.317 (optimization) and according to X-ray data $l_{\mu\nu}$ = 1.367 and 1.367 Å. The closeness of the optimized length of the C(3')–C(4') single bond $l_{\mu\nu}$ = 1.410 Å to that obtained by the X-ray method ($l_{\mu\nu}$ = 1.434 Å) is noteworthy. No significant differences were observed in the calculated bond lengths in the oxazole and furan rings in the *cis* and *trans* conformers of the **FO** molecule, although in *trans*-**FO** the C(2)–C(2') single interring bond was somewhat longer ($l_{\mu\nu}$ = 1.460 Å) than in *cis*-**FO** ($l_{\mu\nu}$ = 1.439 Å). In both conformers this bond has approximately the same order ($p_{\mu\nu}$ = 0.303 and 0.301). The length of the C(2)–C(2') bond in *trans*-**FO** according to X-ray data is $l_{\mu\nu}$ = 1.459 Å (Table 6).

TABLE 6. Lengths $l_{\mu\nu}$* and Bond Orders $p_{\mu\nu}$ in 2-(2-Furyl)- and 2-(2-Thienyl)oxazole according to Data of the PPP/S and INDO/S Methods

Com-pound	Conformation (method of calculation)	Parameter (state)*	O(1)–C(2)	C(2)–N(3)	N(3)–C(4)	C(4)–C(5)	C(5)–O(1)	C(2)–C(2')	C(2')–O(1) or S(1')–C(2')	C(2')–C(3')	C(3')–C(4')	C(4')–C(5')	C(5')–O(1') or C(5')–S(1')
1	2	3	4	5	6	7	8	9	10	11	12	13	14
2-(2-Furyl)-oxazole	*cis*-**FO** (PPP/S)	$l_{\mu\nu}$	1.315	1.322	1.347	1.376	1.322	1.439	1.323	1.384	1.410	1.378	1.319
		$p_{\mu\nu}$ (S_0)	0.483	0.706	0.567	0.781	0.440	0.303	0.435	0.736	0.583	0.768	0.463
		$p_{\mu\nu}$ (S_1*)	0.312	0.445	0.636	0.650	0.405	0.581	0.331	0.462	0.665	0.673	0.384
		$\Delta p_{\mu\nu}$, %	13.5	14.3	-4.2	6.5	3.1	18.5	9.2	14.4	4.8	4.8	6.6
		$p_{\mu\nu}$ (S_2*)	0.171	0.261	0.069	0.131	0.035	0.278	0.104	0.274	0.082	0.095	0.079
		$p_{\mu\nu}$ (S_3*)	0.422	0.624	0.564	0.726	0.414	0.401	0.33	0.530	0.371	0.448	0.397
		$p_{\mu\nu}$ (S_4*)	0.352	0.558	0.427	0.544	0.383	0.359	0.440	0.517	0.555	0.712	0.373
		$p_{\mu\nu}$ (T_1)	0.377	0.554	0.624	0.647	0.385	0.470	0.323	0.441	0.639	0.599	0.345
		$\Delta p_{\mu\nu}$, %	9.1	9.0	3.8	7.2	5.2	14.8	10.8	16.7	3.7	9.2	10.6
		$p_{\mu\nu}$ (T_2)	0.361	0.661	0.611	0.390	0.336	0.260	0.375	0.375	0.603	0.562	0.389
		$p_{\mu\nu}$ (T_3)	0.462	0.668	0.529	0.693	0.434	0.362	0.366	0.366	0.342	0.453	0.390
		$p_{\mu\nu}$ (T_4)	0.438	0.318	0.393	0.546	0.403	0.307	0.426	0.426	0.551	0.768	0.430
		$p_{\mu\nu}$ (T_5)	0.333	0.437	0.165	0.641	0.509	0.376	0.391	0.391	0.517	0.716	0.461
		$p_{\mu\nu}$ (T_6)	0.421	0.626	0.478	0.730	0.436	0.372	0.323	0.323	0.171	0.445	0.595
	trans-**FO** (PPP/S)	$l_{\mu\nu}$	1.314	1.323	1.347	1.377	1.321	1.460	1.321	1.385	1.410	1.379	1.317
		$p_{\mu\nu}$ (S_0)	0.492	0.699	0.569	0.778	0.449	0.301	0.450	0.731	0.585	0.765	0.472
		$p_{\mu\nu}$ (S_1*)	0.319	0.448	0.635	0.636	0.419	0.581	0.334	0.459	0.658	0.675	0.400
		$\Delta p_{\mu\nu}$, %	13.8	14.0	4.1	7.1	2.6	18.8	10.1	14.6	4.3	4.6	6.0
		$p_{\mu\nu}$ (S_2*)	0.427	0.617	0.561	0.720	0.422	0.394	0.337	0.530	0.377	0.454	0.406
		$p_{\mu\nu}$ (S_3*)	0.386	0.560	0.448	0.556	0.389	0.362	0.453	0.493	0.551	0.692	0.376
		$p_{\mu\nu}$ (T_1)	0.381	0.545	0.628	0.640	0.390	0.472	0.332	0.441	0.639	0.603	0.356
		$\Delta p_{\mu\nu}$, %	9.4	9.1	4.0	7.3	5.4	15.0	10.9	16.5	35.2	8.8	10.2
		$p_{\mu\nu}$ (T_2)	0.373	0.628	0.611	0.395	0.341	0.258	0.386	0.656	0.605	0.554	0.393
		$p_{\mu\nu}$ (T_3)	0.471	0.658	0.528	0.672	0.445	0.361	0.383	0.500	0.353	0.447	0.405
		$p_{\mu\nu}$ (T_4)	0.447	0.337	0.405	0.530	0.422	0.304	0.438	0.595	0.542	0.767	0.434
		$p_{\mu\nu}$ (T_5)	0.372	0.475	0.276	0.713	0.468	0.381	0.469	0.615	0.431	0.648	0.508
		$p_{\mu\nu}$ (T_6)	0.397	0.578	0.369	0.689	0.474	0.371	0.350	0.571	0.275	0.531	0.559
	trans-**FO** (INDO/S)	$l_{\mu\nu}$[a]	1.360	1.294	1.384	1.347	1.378	1.459	1.367	1.343	1.434	1.343	1.367
		$p_{\mu\nu}$ (S_0)	0.060	0.225	0.155	0.264	0.045	0.032	0.032	0.280	0.100	0.308	0.043
		$p_{\mu\nu}$ (S_1*) ($\pi\pi$*)	-0.158	-0.260	0.099	0.165	-0.048	0.268	-0.085	-0.263	0.101	-0.107	-0.057
		$p_{\mu\nu}$ (T_1) ($\pi\pi$*)	-0.164	-0.232	0.144	-0.289	-0.112	0.149	-0.044	-0.182	0.046	-0.071	-0.049

TABLE 6 (continued)

1	2	3	4	5	6	7	8	9	10	11	12	13	14
2-(2-Thienyl)-oxazole	*cis*-**TO** (PPP/S)	$l_{\mu\nu}$	1.315	1.324	1.346	1.378	1.321	1.455	1.757	1.364	1.440	1.355	1.755
		$p_{\mu\nu}$ (S_0)	0.485	0.696	0.575	0.773	0.450	0.329	0.196	0.853	0.412	0.900	0.205
		$p_{\mu\nu}$ (S_1^*)	0.382	0.520	0.633	0.653	0.439	0.577	0.091	0.501	0.594	0.706	0.177
		$p_{\mu\nu}$ (S_2^*)	0.456	0.652	0.566	0.771	0.423	0.411	0.127	0.617	0.419	0.688	0.204
		$p_{\mu\nu}$ (S_3^*)	0.396	0.594	0.541	0.616	0.398	0.345	0.233	0.577	0.522	0.720	0.022
		$p_{\mu\nu}$ (S_4^*)	0.348	0.531	0.584	0.642	0.455	0.365	0.110	0.679	0.422	0.601	0.188
		$p_{\mu\nu}$ (T_1)	0.451	0.642	0.588	0.750	0.436	0.431	0.111	0.426	0.595	0.550	0.116
		$p_{\mu\nu}$ (T_2)	0.347	0.543	0.654	0.492	0.341	0.386	0.160	0.806	0.361	0.603	0.177
		$p_{\mu\nu}$ (T_3)	0.421	0.689	0.565	0.522	0.399	0.306	0.190	0.528	0.288	0.676	0.187
		$p_{\mu\nu}$ (T_4)	0.448	0.311	0.377	0.501	0.400	0.333	0.130	0.766	0.416	0.889	0.185
		$p_{\mu\nu}$ (T_9)	0.352	0.502	0.166	0.585	0.534	0.423	0.134	0.740	0.434	0.832	0.174
		$p_{\mu\nu}$ (T_{10})	0.447	0.615	0.489	0.765	0.434	0.402	0.085	0.641	0.452	0.712	0.151
	trans-**TO** (PPP/S)	$l_{\mu\nu}$	1.315	1.324	1.346	1.377	1.321	1.455	1.760	1.363	1.441	1.355	1.758
		$p_{\mu\nu}$ (S_0)	0.483	0.697	0.571	0.776	0.446	0.328	0.181	0.850	0.410	0.902	0.193
		$p_{\mu\nu}$ (S_1^*)	0.383	0.518	0.630	0.664	0.435	0.577	0.093	0.501	0.598	0.700	0.154
		$p_{\mu\nu}$ (S_2^*)	0.450	0.647	0.568	0.764	0.418	0.410	0.111	0.620	0.398	0.640	0.252
		$p_{\mu\nu}$ (S_3^*)	0.393	0.602	0.530	0.617	0.399	0.346	0.254	0.585	0.534	0.534	0.741
		$p_{\mu\nu}$ (S_4^*)	0.338	0.513	0.593	0.646	0.446	0.354	0.091	0.688	0.426	0.629	0.184
		$p_{\mu\nu}$ (T_1)	0.452	0.638	0.592	0.746	0.439	0.433	0.119	0.425	0.596	0.552	0.124
		$p_{\mu\nu}$ (T_2)	0.348	0.536	0.659	0.494	0.341	0.386	0.173	0.805	0.365	0.602	0.186
		$p_{\mu\nu}$ (T_3)	0.451	0.684	0.572	0.532	0.401	0.303	0.206	0.519	0.288	0.673	0.197
		$p_{\mu\nu}$ (T_4)	0.466	0.335	0.377	0.473	0.409	0.339	0.207	0.764	0.419	0.887	0.194
		$p_{\mu\nu}$ (T_5)	0.341	0.652	0.561	0.781	0.423	0.390	0.040	0.614	0.460	0.695	0.144
		$p_{\mu\nu}$ (T_6)	0.396	0.460	0.093	0.577	0.546	0.432	0.168	0.754	0.436	0.874	0.178
	trans-**TO** (INDO/S)	$l_{\mu\nu}{}^a$	1.360	1.294	1.384	1.347	1.378	1.490	1.720	1.343	1.440	1.343	1.720
		$p_{\mu\nu}$ (S_0)	1.056	1.267	1.094	1.313	1.031	1.025	1.020	1.310	1.078	1.334	1.034
		$p_{\mu\nu}$ $(S_1^*)(\pi\pi^*)$	-0.152	-0.234	0.110	-0.175	-0.003	0.268	-0.092	-0.271	0.121	-0.132	-0.035
		$p_{\mu\nu}$ (T_1) $(\pi\pi^*)$	-0.071	-0.113	0.100	-0.128	-0.030	0.139	-0.088	-0.340	0.161	-0.263	-0.092

* $l_{\mu\nu}$ is the bond length obtained by optimizing the geometry by the PPP/S method; $l_{\mu\nu}{}^a$ is the bond length from experimental data (X-ray analysis, electronography, microwave spectra) for the related compounds [9,11-13].

The bond lengths calculated by the PPP/S method in the oxazole ring of the *cis* and *trans* isomers of **TO** are close to those given for **FO**. The lengths ($l_{\mu\nu}$ = 1.757 and 1.755 Å) of the S(1')–C(2) and C(5)–S(1') single ($p_{\mu\nu}$ = 0.181-0.205) bonds in the thiophene ring are somewhat overestimated compared with the experimental value ($l_{\mu\nu}$ = 1.720 Å) for the analogs, but attention is drawn by the coincidence with X-ray data of the optimized length of the single C(3')–C(4') bond ($l_{\mu\nu}$ = 1.440 Å). The lengths of the double C(2')=C(3') and C(4')=C(5') bonds ($l_{\mu\nu}$ = 1.363 and 1.355 Å optimized by PPP/S, and $l_{\mu\nu}$ = 1.363 Å for each bond by X-ray) also differed insignificantly. The higher order of the C(2')=C(3') and C(4')=C(5') double bonds in the thiophene ring of **TO** ($p_{\mu\nu}$ = 0.850 and 0.902) compared with the analogous bonds in the furan ring of **FO** ($p_{\mu\nu}$ = 0.736 and 0.768) should be mentioned. In *cis*- and *trans*-**TO** the lengths of the single C(2)–C(2') interring bonds were the same ($l_{\mu\nu}$ = 1.455 Å, $p_{\mu\nu}$ = 0.328). The C(2)–C(2') bond length in *trans*-**TO** is $l_{\mu\nu}$ = 1.490 Å according to X-ray data (Table 6).

A redistribution of bond orders $p_{\mu\nu}$ occurs on exciting the molecules according to the PPP/S and INDO/S calculations. The orders of the single bonds in the ground state are increased, but the orders of the double bonds are reduced. The change in order of the C(2)–C(2') interring bond is particularly significant in the transitions $S_0 \rightarrow S_1$* and $T_1 \rightarrow S_0$. According to the PPP/S method, $p_{\mu\nu}$ = 0.303 for *cis(trans)*-**FO** in the S_0 state, $p_{\mu\nu}$* = 0.581 in the fluorescent S_1* state, and $p_{\mu\nu}$* = 0.470 (0.472) in the T_1 state, but for *cis(trans)*-**TO** $p_{\mu\nu}$ = 0.328 (0.329) (S_0), $p_{\mu\nu}$* = 0.577 (S_1*), and $p_{\mu\nu}$* = 0.431 (0.433) (T_1) respectively. This indicates an increase in the interaction of the $\sigma\pi$ electronic subsystems of the rings in the excited states compared with the ground state, in which the rings are quasi-independent, especially in the *trans* conformation.

The change in the order of the C(2)–C(2') inter-ring bond corresponding to the formation of the electronic-vibrational structure of the LAB in the UV absorption and fluorescence spectra was confirmed experimentally by the low-temperature spectra of certain polycyclic azoles containing the same subsystems and also by quantum chemical methods [14,15]. Analysis of the electronic-vibrational structure of the fluorescence and phosphorescence bands in the vapor and in solution showed that in the excited states the molecules investigated must have a coplanar orientation of the rings. In the ground state the most stable are the conformers with the rings twisted by an angle φ = 24-45° [9]. This enabled the application of the PPP/S method to the calculation of photophysical properties of heterocyclic molecules to be proved in an orderly manner [1-4].

It should be noted that, according to the data of PPP/S calculations, on excitation of *cis(trans)*-**FO** the orders of one single and two double bonds are changed markedly. The O(1)–C(2), C(2)–N(3), and C(4)–C(5) bonds in the oxazole ring are changed from $p_{\mu\nu}$ = 0.483 (0.492), 0.706 (0.699), and 0.781 (0.778) in the S_0 state to $p_{\mu\nu}$* = 0.312 (0.319), 0.445 (0.448), and 0.650 (0.636) in the fluorescent S_1* state, and also to $p_{\mu\nu}$* = 0.377 (0.381), 0.554 (0.545), and 0.647 (0.640) in the T_1 state. The bond orders in the furan ring depend markedly on the spin and conformation of the molecule. In *cis(trans)*-**FO** the bond orders of O(1')–C(2'), C(2')–C(3'), C(4')–C(5'), and O(1')-C(5') are changed from $p_{\mu\nu}$ = 0.435 (0.450), 0.736 (0.731), 0.768 (0.765), and 0.463 (0.472) (S_0) to $p_{\mu\nu}$* = 0.331 (0.334), 0.462 (0.459), 0.673 (0.658), and 0.384 (0.400) (S_1*) and $p_{\mu\nu}$* = 0.327 (0.332), 0.441 (0.441), 0.559 (0.603), and 0.345 (0.356) (T_1). We note the large increase of the C(3')–C(4') bond order in the furan ring for *cis*- and *trans*-**FO** (to $p_{\mu\nu}$ = 0.639) in the T_1 state compared with the S_0 state ($p_{\mu\nu}$ = 0.583 and 0.585 respectively). Activation of electronic-vibrational processes in the furan ring is therefore observed in the T_1 triplet state, the overall change of bond orders $\Delta p_{\mu\nu}$* = 51 (81.6)% for *cis(trans)*-**FO**. The data from the INDO/S method indicate a similar character for the changes in $\Delta p_{\mu\nu}$* (Table 6).

In the excited states of *cis*- and *trans*-**TO** the O(1)–C(2), C(2)–N(3), and C(4)–C(5) bond orders in the oxazole ring are changed markedly from $p_{\mu\nu}$ = 0.483 (0.485), 0.697 (0.695), and 0.776 (0.773) in the S_0 state to $p_{\mu\nu}$* = 0.383 (0.382), 0.518 (0.520), and 0.664 (0.653) in the fluorescent S_1* state. The changes in bond order in the T_1 state are significantly less, to $p_{\mu\nu}$* = 0.451 (0.452), 0.642 (0.638), and 0.750 (0.746). In the thiophene ring the changes in bond order depend markedly on the spin and conformation of the molecule. On exciting **TO** the S(1')–C(2') (greatest change in the S_1* state), C(2')–C(3') (greatest change in the T_1 state), and C(5')–S(1') bonds are shortened, but the C(3')–C(4') bond is lengthened. The orders of the indicated bonds for *cis(trans)*-**TO** are changed respectively from $p_{\mu\nu}$ = 0.181 (0.196), 0.850 (0.853), 0.410 (0.412), and 0.193 (0.205) (S_0) to

$p_{\mu\nu}$* = 0.093 (0.091), 0.501 (0.501), 0.598 (0.594), and 0.154 (0.177) (S_1*) and $p_{\mu\nu}$* = 0.111 (0.119), 0.426 (0.425), 0.595 (0.596), and 0.116 (0.124) (T_1). This means that in the phosphorescent state both *cis*- and *trans*-**TO** are characterized by activation of the electronic-vibrational processes in the thiophene ring, the overall change in bond orders is $\Delta p_{\mu\nu}$* = 80.8 to 88.6% (somewhat less in the fluorescent state $\Delta p_{\mu\nu}$* = 58.5 to 63.1 %).

Thus, we have studied the interconnection of structure and electronic-vibrational processes in 2-(2-furyl)- and 2-(2-thienyl)oxazoles with their chemical reactivity. The quantum-chemical and spectral characteristics obtained enable the direction of substitution reactions in these systems to be predicted on the basis of the degree of localization and delocalization of the electronic-vibrational excitation, and may be used for the synthesis of needed compounds.

REFERENCES

1. A. E. Obukhov and L. I. Belen'kii, *Khim. Geterotsikl. Soedin.*, 1181 (1998).
2. A. E. Obukhov and L. I. Belen'kii, *Khim. Geterotsikl. Soedin.*, 948 (1999).
3. A. E. Obukhov, *Laser Physics*, **7**, 1102 (1997).
4. L. I. Belen'kii, M. A. Cheskis, V. P. Zvolinskii, and A. E. Obukhov, *Khim. Geterotsikl. Soedin.*, 826 (1986).
5. L. I. Belen'kii and M. A. Cheskis, *Khim. Geterotsikl. Soedin.*, 881 (1984).
6. L. I. Belen'kii, G. P. Gromova, M. A. Cheskis, and Ya. L. Gol'dfarb, *Chem. Scripta*, **25**, 295 (1985).
7. L. I. Belen'kii, V. S. Bogdanov, I. A. Abronin, G. P. Gromova, M. A. Cheskis, and R. Z. Zakharyan, *Chem. Scripta*, **25**, 266 (1985).
8. L. I. Belen'kii and N. D. Chuvylkin, *Khim. Geterotsikl. Soedin.*, 1535 (1996).
9. N. I. Popik, M. V. Shablygin, L. V. Vilkov, A. S. Semenova, and T. V. Kravchenko, *Vysokomol. Soedin.*, **25B**, 38 (1983).
10. A. E. Obukhov, *Laser Physics*, **9**, 927 (1999).
11. A. I. Kitaigorodskii, P. M. Zorkii, and V. K. Bel'skii, *Structure of Organic Substances. Data of X-ray Structural Investigations* [in Russian], Nauka, Moscow (1980), chap. 1, p. 647.
12. B. Bak, D. Christensen, L. Hansen-Nygaard, and J. Rastrup-Andersen, *J. Mol. Spectrosc.*, **7**, 58 (1961).
13. R. A. Bonham and F. A. Momany, *J. Phys. Chem.*, **67**, 2474 (1963).
14. A. E. Obukhov, *Laser Physics*, **9**, 699 (1999).
15. A. E. Obukhov, *Laser Physics*, **9**, 723 (1999).